Imaging of Electrically Detected Magnetic Resonance of a Silicon Wafer

Toshiyuki Sato,* Hidekatsu Yokoyama,†,1 Hiroaki Ohya,† and Hitoshi Kamada†

*Yamagata Research Institute of Technology, Yamagata 990-2473, Japan; and †Institute for Life Support Technology,
Yamagata Public Corporation for Development of Industry, Yamagata 990-2473, Japan

An imaging technique of electrically detected magnetic resonance (EDMR) was newly developed. Because the EDMR signal is obtained from paramagnetic recombination centers, one may expect the image to represent the distribution of defect and/or impurity sites in the sample. We successfully obtained EDMR images of a light-illuminated silicon plate 8 mm in width and 15 mm in length, which was cut from a silicon wafer (n-type, $100 \, \Omega$ cm), under ESR irradiation at a frequency of 890 MHz (wavelength, 340 mm). The reproducibility of the EDMR image obtained from a sample was amply satisfactory. When the oxidized surface of the silicon was removed, the EDMR signal disappeared. Although the EDMR signal reappeared when the surface of the sample became reoxidized, the EDMR image obtained was slightly different from the earlier one. This finding shows that the EDMR image obtained from the sample shows the distribution of defects at the Si/SiO$_2$ interface. © 2001 Academic Press

Key Words: EDMR; SDR; imaging; loop–gap resonator; UHF; silicon wafer.

INTRODUCTION

Electrically detected magnetic resonance (EDMR) spectroscopy (*1, 2*), also cited as a spin-dependent recombination (SDR), is a method for observing magnetic resonance by detecting the change in electric characteristics, which in most instances is conductivity. With this method, it is possible to detect paramagnetic recombination centers formed by lattice defects or impurities in semiconductor devices with a high sensitivity and selectivity. The technique has been applied to investigate not only semiconductor devices but also other materials (*3, 4*).

The enhancement of EDMR sensitivity has been explained by an electron–hole pair model, where an electron or a hole form a localized pair with a recombination center in a triplet (both spins in the same direction) and a singlet (opposite directions of spin) in a static magnetic field (*5, 6*). The pair in the singlet state is allowed to recombine but the pair in the triplet state is forbidden, so most singlet states will quickly recombine, leaving the system in a triplet rich-state. When recombination centers are irradiated with a microwave under ESR conditions, some triplet

pairs are converted into singlet pairs. Recombination occurs so efficiently under ESR conditions that the enhanced change in electrical properties can be observed.

The pair model also predicts that the relationship between EMDR signal intensity and the static magnetic field strength is not linear. It has been reported that the EDMR sensitivity is constant at a high field (>100 mT) and decreases at a lower field (<4 mT) (*7–9*). Recently, we have clarified this relationship for magnetic fields of 10 to 32 mT, which experimentally bridge the gap between the high- and low-field regions (*10*). Further, we have derived theoretical expressions from a quantum mechanical treatment of the electron–hole pair model (*11*). It was shown that the experimental results support the theory (*3, 11*). At longer microwave lengths, a larger sample space is available, and the skin effect caused by high conductivity of the sample is decreased. Based on the experimental results and simulations, we concluded that around 30 mT was the optimum EDMR field. We have built and evaluated an EDMR instrument operating in the field range (i.e., in the UHF band), where a 44-mm diameter resonator was available (*12*).

Nondestructive observation of the distribution of recombination centers in semiconductors would be very useful, but it is not possible with conventional EDMR or other methods. When the EDMR signal is observed in a gradient field, spatial information on the position of the paramagnetic recombination center in the sample can be obtained. It is therefore possible to obtain an EDMR image by employing a field gradient technique, such as zeugmatography (*13*). In the present study, an EDMR imaging system for visualizing the distribution of paramagnetic recombination centers was developed.

RESULTS AND DISCUSSION

The distributions of EDMR signal intensity for a rectangular silicon plate under uniform light illumination are shown in Figs. 1a–1e. A silicon wafer, used for the sample material, was cut into a rectangular plate and electrodes were formed on both sides as shown in Fig. 1f. When the magnetic field was swept under irradiation at a constant microwave frequency, the photoconductivity decreased under ESR conditions. While field modulation was applied for lock-in detection to improve sensitivity, the differential EDMR spectrum was obtained as a function of

1 To whom correspondence should be addressed. Fax: +81-23-647-3149. E-mail: yokohide@fmu.ac.jp.
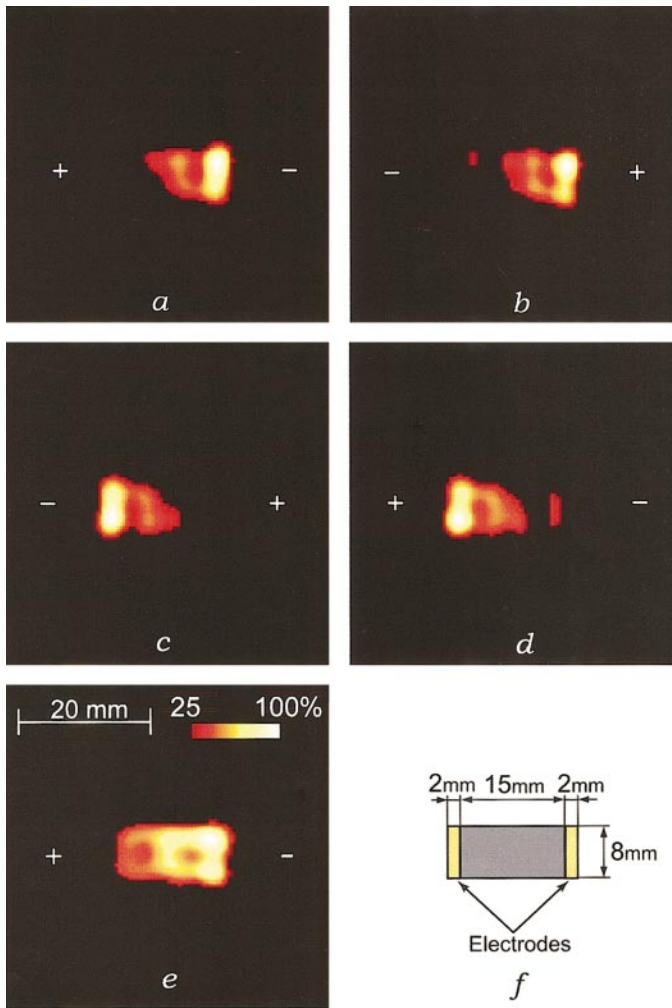
FIG. 1. EDMR images of a silicon rectangular plate (a–e) and its dimensions (f). EDMR images were obtained before etching (a–d). In the pair of (a) and (b), or (c) and (d), the currents were in opposite directions. In the pair of (a) and (c), or (b) and (d) the sample positions were reversed. The EDMR image of the same sample after the oxidized surface was etched and naturally reoxidized is shown in (e). The direction of the sample and the current in (e) and (a) are the same. The silicon rectangular plate, 8 mm in width and 19 mm in length, was cut from the silicon wafer, and the electrodes were attached to both sides of the plate leaving 15 mm free (f).

The directions of current were opposite in Figs. 1a and 1b, and in Figs. 1c and 1d. The polarity applied to the sample is indicated as $+$ and $-$ in the figure. The sample was placed in opposite directions in Figs. 1a and 1c, and in Figs. 1b and 1d. Because the patterns were rotated $180°$ when the direction of a sample was changed, it was proven that uniform illumination of light and an alternative magnetic field, $\mathbf{B_1}$, were applied. The similarity of the EDMR images obtained from the sample also shows that this experiment was highly reproducible. Further, the patterns were the same even when the direction of the current was reversed.

The photo-excited electrons and holes are the dominant carriers in this sample because the concentration of doped impurity is very low in this sample (volume resistance $>100\ \Omega$ cm). The holes move in the same direction as the applied electric field, and the electrons move in the opposite direction. Although the electrons and holes are generated uniformly in the sample under the uniform light illumination, different gradients of concentration between the holes and electrons can be seen in the sample. Different EDMR images might be expected when the polarity is reversed because the density distributions of the conduction electron–recombination center pair or hole–recombination center pair based on the Shockley-Read model (6) could be altered with different electron or hole density distributions. However, such a change was not observed in the present study. Under the experimental conditions described here (with an electrical field of almost 1 V/cm), it is presumed that the diffusion of conduction electrons and holes within the sample overwhelm such distribution gradients, so that no differences in EDMR images would be observed for different polarities.

The current flow could be disturbed by local band bending at the surface of the wafer or a local concentration of recombination centers. However, those influences in this experiment are estimated to be small because most of the carriers go through the bulk area in this sample. The bulk area has enough thickness (0.5 mm) and the carriers are considered to be diffusing uniformly in the area.

When the oxidized surface of silicon was removed by etching, the EDMR signal disappeared; however, it reappeared when the surface of the sample was again oxidized after sitting at the room temperature for some time. This result shows that the EDMR signal was derived from the oxidized surface of silicon. The pattern of the EDMR image from the reoxidized sample, as shown in Fig. 1e, was slightly different from that obtained before etching. The direction of the sample and the current were the same as those in Fig. 1a. These findings show that the EDMR images obtained from the sample indicate the distribution of defects at the Si/SiO$_2$ interface.

In conclusion, a successful EDMR imaging method has been designed, and the 2-D distribution of EDMR signal intensity from a light-illuminated silicon plate has been observed for the first time. This method now enables nondestructive observations of the distribution of paramagnetic recombination centers in semiconductor materials.

the magnetic field. The g value and peak-to-peak linewidth were measured to be 2.005 ± 0.003 and 0.28 mT, respectively. An angular dependence of the sample was not observed. An EDMR image was reconstructed from the spectra where spatial information was convolved by employing a gradient field. The 2-D distribution of the EDMR signal intensity was reconstructed from 18 1-D projections. The full-width at half-maximum (FWHM) of the deconvoluted spectrum that was obtained under a uniform field was measured. The FWHM-to-gradient ratio was used as an index for the spatial resolution (14), which in this study was 1.9 mm.

EXPERIMENTAL

Instrument

A block diagram of an EDMR imaging instrument is shown in Fig. 2. A commercially available resistive magnet (modified RE3X, JEOL, Japan) was used as the main magnet. The static magnetic field, B_0, was set at 31 mT. The magnetic field was scanned by controlling the current in a pair of field scan coils (Helmholtz type coil, Yonezawa Electric Wire, Japan). The sweep time was 1.9 s. Pairs of field gradient coils (Anderson-type coil for the y-gradient and anti-Helmholtz-type coil for the z gradient, Yonezawa Electric Wire) were used to provide a linear field gradient at 2 mT/cm in a range from the center to 20 mm along the y and z axes (15). The magnetic field was modulated at 362 Hz by a pair of modulation coils for lock-in detection. To improve the signal-to-noise ratio, 81 time field sweeps were averaged to obtain one spectrum. The field gradient was applied in the z–y plane, which was rotated by $10°$ after each acquisition of an averaged spectrum. Here the z and x axes are coincident to B_0 and B_1, respectively. The sweep width was set at 15 mT. Under a 2-mT/cm field gradient, data for the 75-mm ($=15$ mT) line in the y and z directions were assigned to 150 data points, i.e., 1 point per 0.5 mm. Among the 150×150 data points, 100×100 points (50×50 mm) of the central fractions were used for the picture. Each 1-D distribution of the EDMR signal intensity was obtained by
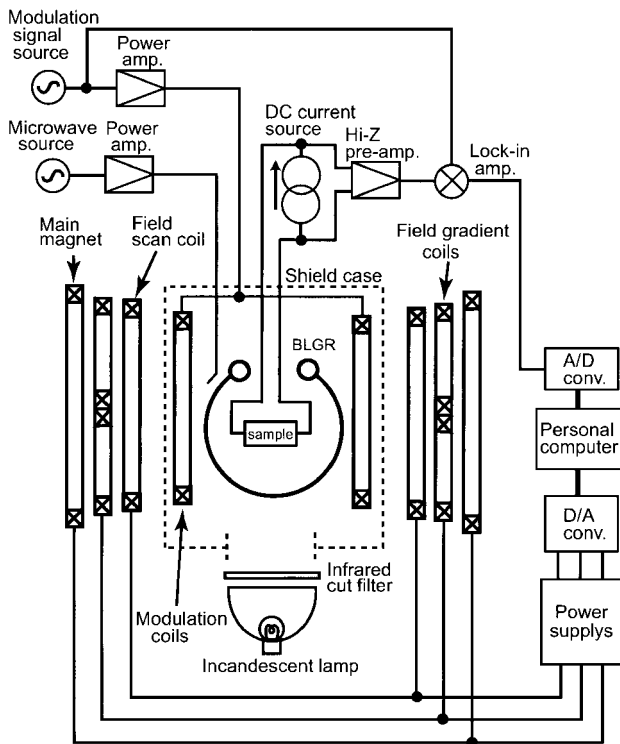
deconvolution of the signals observed in the magnetic field gradient, based on the EDMR spectrum in a uniform field (16). The deconvolution was performed by a fast Fourier transform. The 2-D distribution of the EDMR signal intensity was reconstructed in 256 colors from those 1-D projections. Signals lower than 25% of the maximum signal intensity were regarded as noise.

A synthesized signal generator (MG3633A, Anritsu, Japan; frequency range, 10 kHz–2700 MHz) was used as a microwave source. The microwave power was amplified to 1 W by a power amplifier (A1000-1050, R&K, Japan; gain, 46 dB; output impedance, 50 Ω; bandwidth, 200 MHz to 1 GHz; maximum power, 50 W). The microwave power was below the saturation level (12). A bridged shield loop–gap resonator (BLGR) was used so that B_1 was applied to the sample efficiently and uniformly. The BLGR is known for its large filling factor and homogeneity of the B_1 field (17, 18). The BLGR, a four-gap type, with interior and exterior bridge shields, had a resonant frequency of 890 MHz and a Q value of 510. The bridged shields were located at the gaps via Teflon spacers that were 0.5 mm thick. The diameter of the BLGR, 44 mm with an axial length of 10 mm, was sufficiently short compared to the wavelength (340 mm). Magnetic loop coupling was used so that the coupling could be adjusted by moving the loop along the axis. The BLGR was covered with a shield case so that it prevented radiation from microwave energy and noise penetration.

A DC current source (constructed in our laboratory) and a high input-impedance preamplifier (constructed in our laboratory; input impedance, 9×10^{11} Ω and 1 nF in parallel; gain, 40 dB; bandwidth, 2 Hz to 5 kHz) were used to amplify the change in resistance of a sample (12). They were mounted in a same shield case to reduce the extraneous noise. The sample was biased at 10 μA of the constant current. The lock-in amplifier (5210, PARC, Princeton, NJ; frequency range, 0.5 Hz to 120 kHz) was used to detect the EDMR signal at the modulation frequency. The modulation coils were driven by an internal oscillator in the lock-in amplifier and a power amplifier (4020, NF, Japan; gain, 46 dB). The currents in the scan and gradient coils (for the y and z axes) were from power supplies (NB40-15CS, Stabilizer Co. Ltd., Japan; GP0110-10R and GP060-10R, Takasago Ltd., Japan). The power supplies were controlled by a personal computer (PC9821Xa13, NEC, Japan) via a D/A converter (DAJ98, Canopus Co. Ltd., Japan) and the spectral data were collected via an A/D converter (ADJ98, Canopus), also using the personal computer. A halogen incandescent lamp was used to illuminate the sample. Infrared was inhibited with a glass filter (KG-1; Edmund Optics, Japan; cutoff, 700 nm).

FIG. 2. Block diagram of an EDMR imaging instrument.

Sample

An (100) oriented slice of an n-type 3.5-in. silicon wafer (thickness, 0.5 mm; volume resistance >100 Ωcm), used as
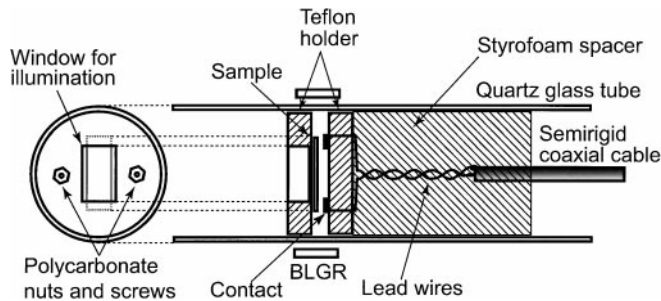
FIG. 3.   Schema of a sample holder for EDMR imaging.

the sample material, was cut into a rectangular plate (width, 8 mm; length, 19 mm). To produce electrodes with ohmic contact, chromium was deposited to a thickness of 400 Å onto the surface of polished silicon, leaving an open area of 15 mm in length (Fig. 1f). Gold was deposited onto the chromium layer to a thickness of 2000 Å. Another surface of the sample, where the electrodes were not constructed, was turned to the axial direction of the BLGR (i.e., the x axis), which was illuminated by the lamp in the same direction. After obtaining the EDMR images, the surface of the wafer was cleaned by using a mixture of sulfuric acid (Kanto Chemicals Co., Inc., Japan), water, and hydrogen peroxide (Kanto) in a volume ratio of 7 : 3 : 1. Subsequently, an aqueous solution of 1% hydrogen fluoride (Kanto) was used to etch off the SiO_2 layer on the sample surface. The EDMR signal could not observed just after the etching operation. After standing in air at room temperature for 72 h, the sample was again oxidized. Then EDMR imaging was performed again.

Sample Holder

The EDMR measurements were performed by using the sample holder shown in Fig. 3. Two Teflon holders (diameter, 33.4 mm; thickness, 5 mm) were set in a quartz glass tube to sandwich the sample. Two polycarbonate screws and nuts fastened the holders together. A 16×9 mm^2 window in the center of one holder allowed light illumination. A pair of gold-plated copper contacts was placed on the other holder, and two copper wires (0.26 mm in diameter) led the electric signal to a semirigid coaxial cable, which was 3.5 cm from the BLGR. The wires were very small so as not to disturb the B_1 in the BLGR. The coaxial cable was connected to the detection circuits (DC current source and high input-impedance preamplifier). A Styrofoam spacer (diameter, 33.5 mm; thickness 48 mm), which was glued to the

Teflon holder, held the pair of wires and the semirigid coaxial cable in place. This spacer was also used to keep the Teflon holders at right angles to the axial direction of the quartz glass tube. The inner and outer diameters of the quartz glass tube were 33.5 and 38 mm, respectively. The glass tube was located at the center of the BLGR.

ACKNOWLEDGMENTS

REFERENCES

1. D. Lepine, *Phys. Rev. B* **6,** 1436 (1972).

2. I. Solomon, *Solid State Commun.* **20,** 215 (1976).

3. T. Eickelkamp, S. Roth, and M. Mehring, *Mol. Phys.* **95,** 967 (1998).

4. A. Maier, A. Grupp, and M. Mehring, *Solid State Commun.* **99,** 623 (1996).

5. D. Kaplan, I. Solomon, and N. F. Mott, *J. Phys. (Paris)* **39,** L51 (1978).

6. F. C. Rong, W. R. Buchwald, E. H. Poindexter, W. L. Warren, and D. J. Keeble, *Solid State Electron.* **34,** 835 (1991).

7. I. Solomon, *Bull. Magn. Reson.* **5,** 119 (1983).

8. R. L. Vranch, B. Henderson, and M. Pepper, *Appl. Phys. Lett.* **52,** 1161–1163 (1987).

9. M. S. Brandt, M. W. Bayerl, N. M. Reinacher, T. Wimbauer, and M. Stutzmann, *Mater. Sci. Fourum* **258–263,** 963–968 (1997).

10. T. Sato, H. Yokoyama, H. Ohya, and H. Kamada, *J. Magn. Reson.* **139,** 422–429 (1999).

11. K. Fukui, T. Sato, H. Yokoyama, H. Ohya, and H. Kamada, *J. Magn. Reson.* **149,** 13–21 (2001).

12. T. Sato, H. Yokoyama, H. Ohya, and H. Kamada, *Rev. Sci. Instrum.* **71,** 486–493 (2000).

13. P. C. Lauterbur, *Nature* **242,** 190 (1973).

14. H. Yokoyama, Y. Lin, O. Itoh, Y. Ueda, A. Nakajima, T. Ogata, T. Sato, H. Ohya-Nishiguchi, and H. Kamada, *Free Radical Bio. Med.* **27,** 442–448 (1999).

15. S. Ishida, S. Matsumoto, H. Yokoyama, N. Mori, H. Kumashiro, N. Tsuchihashi, T. Ogata, M. Yamada, M. Ono, T. Kitajima, H. Kamada, and E. Yoshida, *Magn. Reson. Imaging* **10,** 21–27 (1992).

16. P. A. Jansson, "Deconvolution with Application in Spectroscopy," Academic Press, New York (1984).

17. M. Ono, T. Ogata, K. Hsieh, M. Suzuki, E. Yoshida, and H. Kamada, *Chem. Lett.* 491–494 (1986).

18. H. Hirata, H. Iwai, and M. Ono, *Rev. Sci. Instrum.* **67,** 73–78 (1996).